# L-BAND RFI IN JAPAN

*Yan Soldo[1,2], Paolo de Matthaeis[1,2] and David M. Le Vine[1]*

[1] NASA, Goddard Space Flight Center, Greenbelt, MD, USA
[2] GESTAR, Goddard Space Flight Center, Greenbelt, MD, USA

## ABSTRACT

In recent years, three instruments have been launched into orbit with the aim of producing global maps of sea surface salinity and soil moisture using the 1400-1427 MHz band: SMOS, Aquarius and SMAP. Although this frequency band is allocated to passive measurements only, RFI (Radio-Frequency Interference) is present in the data of all three missions. On a global scale, the three sensors have observed approximately the same distribution of RFI. Japan is an important exception that has implications for the design of RFI detection algorithms. RFI in Japan is caused by a large number of emitters belonging to the same system (TV receivers) and for this reason some traditional RFI detection strategies detect little to no RFI over Japan. The study of this case has led to an improvement of the approach to detect RFI in Aquarius data.

***Index Terms***— RFI, Aquarius, SMAP, SMOS

## 1. INTRODUCTION

In the recent years, three missions have been launched with the aim of making global maps of sea surface salinity and/or soil moisture using passive measurements of Earth's emissions within the 1400-1427 MHz band. These missions are: SMOS (Soil Moisture and Ocean Salinity) operated by ESA (European Space Agency) [1]; Aquarius onboard Aquarius/SAC-D observatory, which is a collaboration between NASA (National Aeronautics and Space Administration) and CONAE (Comisión Nacional de Actividades Espaciales) [2]; and SMAP (Soil Moisture Active/Passive) operated by NASA [3].

Although these missions have passive instruments operating in a frequency range that is allocated to passive measurements only, RFI (Radio-Frequency Interference) is present in the data of all three missions, and each team has put significant effort to cope with this issue.

## 2. HISTORICAL BACKGROUND

Japan, as seen by SMOS, had only moderate levels of RFI contamination until the end of September 2011. Then, between September 21st and September 27th, RFI suddenly appeared in large portions of the country and is still present today.

Aquarius, which had started acquiring measurements shortly before this event, recorded a sudden increase in the average antenna temperatures ($T_A$) measured over Japan around the same time. This increase is clearly visible in the time series of $T_A$ over the major Japanese cities. Figure 1 shows the $T_A$ (average of V- and H-polarization) over Nagoya for the period September 2011 to October 2012 as measured by two of the Aquarius radiometers. Each data point is an average within a 50 km radius centered over the city of Nagoya. Figure 1 also shows the time series of expected antenna temperatures (dashed lines). These values are distributed as part of the Aquarius product and they are computed from models of land and ocean emissivity and ancillary meteorological data. The expected values remain relatively constant over the entire period. The measured values display a clear increase in September 2011 and again in February 2012. However, this increase in $T_A$ did not correspond to an increase in the level of detected RFI in the Aquarius processing.

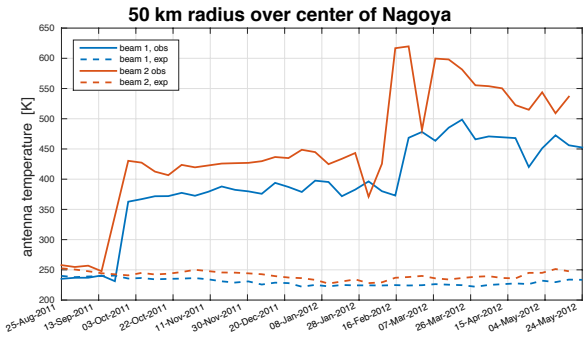


**Fig. 1**. Evolution of the average Aquarius $T_A$ over Nagoya for the first year of measurements. Two steps are clearly visible at the end of September 2011 and in mid-February 2012.

## 3. RFI CHARACTERISTICS OBSERVED FROM REMOTE SENSING DATA

In order to understand why the level of detected RFI did not increase in Aquarius, and to consider ways to improve its RFI detection strategy, the RFI in Japan was studied using all available sensors. Together, data from SMOS, Aquarius

and SMAP, allows one to retrieve information about the RFI, which can be used to assess which approach works best to detect RFI of this kind.

### 3.1. Time domain

Aquarius and SMAP provide data on short time intervals: 10 ms for Aquarius [4] and 300 µs for SMAP [5]. However, even with these high temporal sampling rates, the RFI in Japan does not create obvious outliers in the time series of measured antenna temperatures. Rather, the mean measured antenna temperatures vary slowly, similar to what is expected near coastlines. Figure 2 shows an example from Aquarius. Although the values of $T_A$ (bottom panel) indicate the presence of RFI, there are no outliers in the time series of 10 ms short accumulations (top panel) that is used for RFI detection. In fact, the time-domain outlier detection algorithm used in Aquarius and SMAP detect only few samples as RFI.

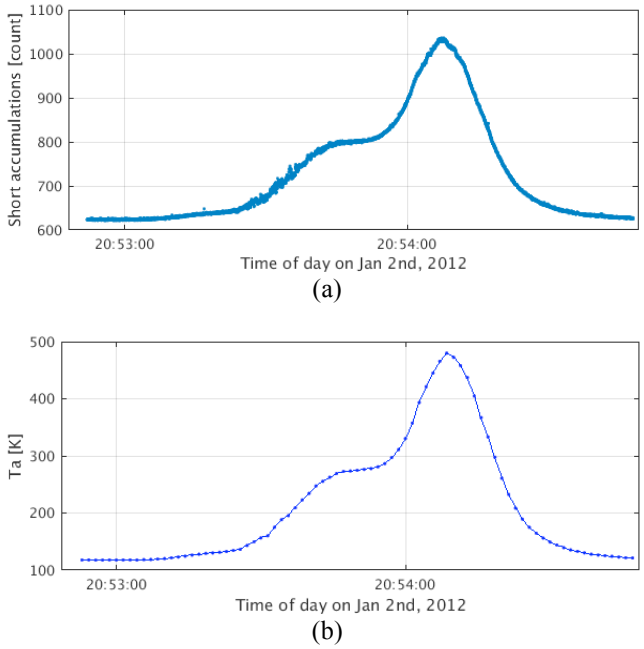


**Fig. 2**. Time series of the 10-ms short accumulations (a) and the corresponding antenna temperatures (b) measured by the Aquarius middle beam on January 2nd, 2012, during an orbit over Nagoya, Japan. Even though $T_A$ higher than 400 K indicate the presence of RFI, there are no obvious outliers in either time series.

### 3.2. Frequency domain

SMAP also provides the possibility to characterize the RFI emissions in frequency by dividing the received signal into 16 spectral sub-bands. Figure 3 shows the amplitude of the measured $T_A$ as a function of frequency, for the city of Osaka during one orbit on June 1st, 2015. $T_A$ is high towards both edges of the protected band with little to no RFI contamination at the center of the band. Also, the amplitude of $T_A$ is approximately the same on both ends of the protected band.

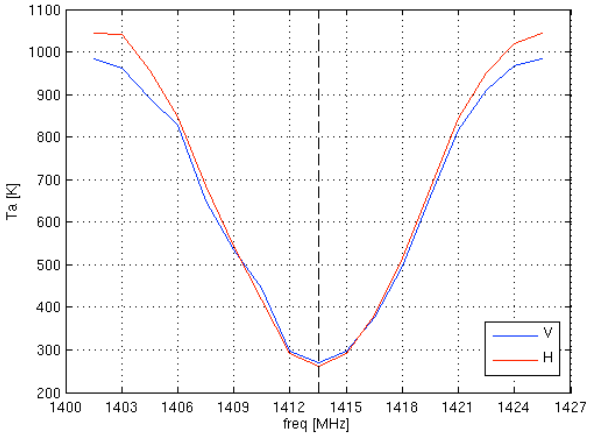


**Fig. 3**. Average SMAP $T_A$ over Osaka as a function of frequency. The central sub-band (at 1413.5 MHz) has $T_A$ consistent with natural emissions, while both ends have a significantly higher level and are clearly affected by RFI.

### 3.3. Horizontal and vertical polarizations

The presence of RFI increases the signal received by real-aperture radiometers. This leads to brightness temperatures that are higher than the level expected from natural emissions alone. In SMOS, which employs a synthetic aperture radiometer, the RFI signal can both increase and decrease the retrieved brightness temperatures in the image [6].

SMOS is able to detect this particular type of RFI by comparing the measured brightness temperatures with thresholds based on the minimum and maximum level of brightness temperature expected from the natural emissions. However, a similar approach is not applied in SMAP and Aquarius RFI algorithms.

### 3.4. Third and fourth Stokes parameters

The 3rd and 4th Stokes parameters have been considered for the detection of RFI [7, 8] as they are expected to be close to zero for emissions from natural targets [9, 10]. The Japanese RFI is not clearly visible from measurements of the 3rd Stokes parameter. The 4th Stokes parameter measurements provided by SMOS and SMAP are also difficult to exploit as they are affected by significant noise and by the vicinity with coastlines.

### 3.5. Kurtosis and skewness

Other RFI detection approaches are based on the statistical distribution of the measured $T_A$. These approaches measure the kurtosis of the incoming signal and compare it with the value expected from a normal distribution (equal to three) [9, 12]. The skewness has not been considered to detect RFI, but it is also an indicator that describes the shape of the

statistical distribution, and therefore it could also be used to detect anomalies.

However, both the kurtosis and the skewness computed from the statistical moments provided in SMAP L1A data do not show any appreciable deviation from the Gaussian values over Japan. As far as the statistical distribution is concerned, this RFI appears as if it were a thermal source (its distribution is Gaussian), only warmer.

## 4. IMPROVEMENT OF THE RFI DETECTION STRATEGY IN AQUARIUS

In many aspects (statistical distribution, 3rd and 4th Stokes parameters, time series), the RFI in Japan presents the characteristics of thermal noise and it is therefore difficult to detect with the outlier detection algorithm implemented in Aquarius [11]. Two criteria are able to correctly detect this RFI: the cross-frequency outlier detection (used in SMAP), and comparing the measurements with thresholds based on the expected natural emission (used in SMOS). The former, however, cannot be implemented in Aquarius since the received signal is not filtered into different sub-band; also, it is possible that if the RFI signal had a uniform spectrum within the protected band, even this approach might not be able to detect it.

In order to improve RFI detection, the Aquarius algorithm can compare the measured antenna temperatures against a threshold, based on the highest antenna temperature expected from the natural scene. This threshold is obtained assuming an ideal surface (flat, homogeneous with no vegetation layer) and using the Mironov model [12] for the dielectric constant of soil and assuming perfectly dry soil (zero soil moisture). To establish an upper limit, the thermodynamic temperature is assumed to be 340 K. If the observed antenna temperature exceeds that computed for this surface in the Aquarius simulator, a flag will be raised.

Figure 4 shows the percent of measurements flagged as RFI: by Aquarius outlier detection algorithm (b), by Aquarius, after adding the comparison with a fixed threshold (c) and by SMOS (c).

Implementing this additional detection algorithm in Aquarius increases the level of RFI detected in Japan, and the spatial distribution of detected RFI becomes similar to that of the RFI detected by SMOS.

## 5. SUMMARY AND CONCLUSIONS

The RFI in Japan affects measurements from all three passive L-band satellites. While most RFI are caused by individual emitters, the Japanese RFI is caused by a large number of emitters belonging to the same system and therefore with the same characteristics. Experiments in 2015 indicated a TV broadcast system as the source of RFI and pointed to an intermediate frequency in the TV receiver as the source.

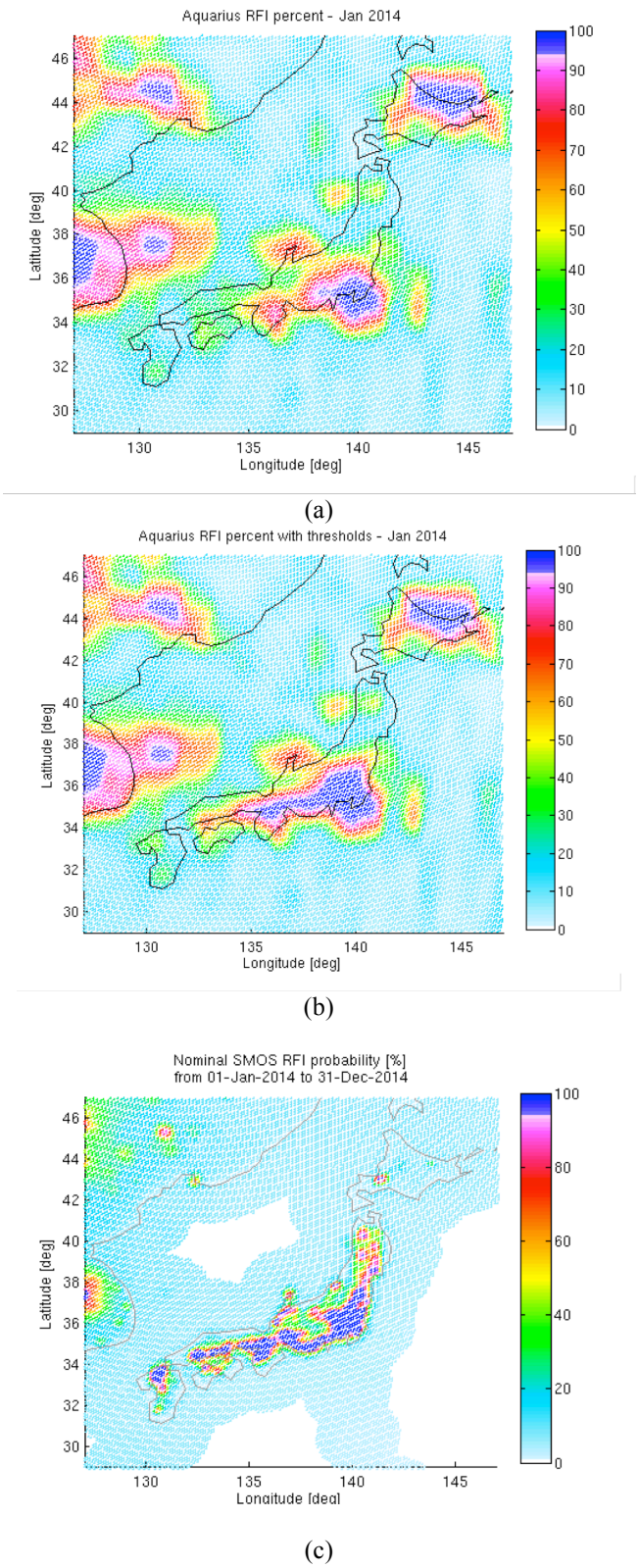


**Fig. 4**. Percent of measurements flagged as RFI over Japan [%]. (a) Aquarius outlier detection algorithm; (b) Aquarius outlier detection algorithm and thresholds; (c) SMOS.

These small independent signals appear to add up randomly resulting in a total contribution that is: a) of a significant level, and b) has the characteristics of thermal noise. Hence, outlier detectors such as those employed by Aquarius and kurtosis detectors such as on SMAP fail to detect RFI even though the level is substantially above the value one would expect from a natural surface. SMOS employs a threshold detection algorithm, which detected the change in RFI, and SMAP detects RFI due to the particular spectrum of the RFI signal.

This analysis has led to the addition of an extra criterion to detect interference in the Aquarius processing. In particular, a threshold option has been added to the criterion for detecting RFI. In the next release of Aquarius data, RFI will also be detected by comparing the measured antenna temperatures against an absolute threshold based on the maximum expected level of natural emissions.

## 6. REFERENCES


[1] Y.H. Kerr, P. Waldteufel, J.-P. Wigneron, J.M. Martinuzzi, J. Font, M. and Berger, "Soil moisture retrieval from space: The Soil Moisture and Ocean Salinity (SMOS) mission," *IEEE Transactions on Geoscience and Remote Sensing*, vol. 39, pp. 1729-1735, 2001.

[2] D.M. Le Vine, G.S.E. Lagerloef, F.R. Colomb, S.H. Yueh and F. Pellerano, "Aquarius: An instrument to monitor sea surface salinity from space," *IEEE Transactions on Geoscience and Remote Sensing*, vol. 45, pp. 2040-2050, 2007. Y.H. Kerr, P. Waldteufel, J.-P. Wigneron, J.M. Martinuzzi, J. Font, M. and Berger, "Soil moisture retrieval from space: The Soil Moisture and Ocean Salinity (SMOS) mission," *IEEE Transactions on Geoscience and Remote Sensing*, vol. 39, pp. 1729-1735, 2001.

[3] D. Entekhabi, E.G. Njoku, P.E. Neill, K.H. Kellogg, W.T. Crow, W.N. Edelstein, J.K. Entin, S.D. Goodman, T.J. Jackson, J.T. Johnson and J. Kimball, "The soil moisture active passive (SMAP) mission," *Proceedings of the IEEE*, vol. 98, pp. 704-716, 2010.

[4] D.M. Le Vine, G.S.E. Lagerloef and S.E. Torrusio, "Aquarius and remote sensing of sea surface salinity from space," *Proceedings of the IEEE*, vol. 98, pp. 688-703, 2010.

[5] J.R. Piepmeier, J.T. Johnson, P.N. Mohammed, D. Bradley, C.S. Ruf, M. Aksoy, R. Garcia, D. Hudson, L. Miles and M. Wong, "Radio-frequency interference mitigation for the soil moisture active passive microwave radiometer," *IEEE Transactions on Geoscience and Remote Sensing*, vol. 52, pp. 761-775, 2014.

[6] Y. Soldo, A. Khazaal, F. Cabot, P. Richaume, A. Anterrieu and Y. H. Kerr, "Mitigation of RFIs for SMOS: A distributed approach," *IEEE Transactions on Geoscience and Remote Sensing*, vol. 52, pp. 7470-7479, 2014.

[7] J.R. Piepmeier, E. Kim, P.N. Mohammed, J. Peng and C.S. Ruf, "*SMAP Calibrated, Time-Ordered Brightness Temperatures L1B_TB Data Product*", Rev. A, 2014.

[8] N. Skou, J.E. Balling, S.S. Sobjarg and S.S. Kristensen, "Surveys and analysis of RFI in the SMOS context," *Proceedings of the 2010 IEEE International Geoscience and Remote Sensing Symposium (IGARSS)*, pp. 2011-2014, 2010.

[9] M. Pardé, M. Zribi, P. Fanise and M. Dechambre, "Analysis of RFI issue using the CAROLS L-band experiment" *IEEE Transactions on Geoscience and Remote Sensing*, vol. 49, pp. 1063-1070, 2011.

[10] A. Khazaal, F. Cabot, E. Anterrieu and Y. Soldo, "A Kurtosis-Based Approach to Detect RFI in SMOS Image Reconstruction Data Processor," *IEEE Transactions on Geoscience and Remote Sensing*, vol. 52, pp. 7038-7047, 2014.

[11] D.M. Le Vine, P. de Matthaeis, C.S. Ruf and D.D. Chen, "Aquarius RFI Detection and Mitigation Algorithm: Assessment and Examples," *IEEE Transactions on Geoscience and Remote Sensing*, vol. 52, pp. 4574-4584, 2014.

[12] V.L. Mironov, L. G. Kosolapova and S. V. Fomin, "Physically and mineralogically based spectroscopic dielectric model for moist soils," *IEEE Transactions on Geoscience and Remote Sensing*, vol. 47, pp. 2059-2070, 2009.